# Minimizing Dwell-Time Conservatism in Supervisory Fault-Tolerant Control: An LMI-Based Approach

M. Gouzien[1,2,†], S. Waitman[2], D. Henry[1]

***Abstract*— This paper addresses the conservatism inherent in dwell-time computation for supervisory fault-tolerant control (FTC) schemes. By leveraging the Multiple Lyapunov Functions (MLF) framework, we establish a formal link with the classical norm-bound approach and propose an iterative LMI-based algorithm to compute the minimal admissible dwell time. The proposed method is validated on the F-8 Crusader aircraft benchmark. A mutual optimization of controller and observer dynamics is conducted, allowing for faster switching and enhanced reconfigurability to faults without compromising global stability. The proposed method allows a $64\%$ reduction in the minimal admissible dwell time computation. Simulations demonstrate a significant improvement in supervisory FTC performance compared to traditional norm-based procedure.**

## I. Introduction

The demand for safety and reliability in modern control systems has driven significant research into Active Fault-Tolerant Control (FTC). Various strategies exist within the FTC community to address these challenges, see [1] for a comprehensive review. FTC methods encompass several paradigms, including supervisory switching such as Multiple Model Switching Control (MMSC) [2], adaptive techniques like Model Reference Adaptive Control (MRAC) [3] or Adaptive Sliding Mode Control [4]. These are often augmented with robustness considerations [5], finite-time convergence properties [6], or Control Allocation (CA) schemes [7].

Despite their versatility, these methods face significant hurdles. For instance, they may require the estimation the fault and/or its location, and they rarely establish stability guarantee during the transient phase [8]. Moreover, no separation principle has been formally established to the best knowledge of the authors, even if the fault diagnosis unit and the control reconfiguration algorithm operate in tight collaboration. One can cite the work reported in [9] that tends to address this issue by using an adaptive gain for the fault estimator combined with an adaptive back-stepping technique.

Based on the theory of supervisory switching control approach initially proposed by [10], a supervisory FTC approach is proposed in [11], [12]. This framework offers a compelling solution for handling intermittent faults and system reconfigurations. A key feature of this approach is the derivation of global (exponential) stability conditions based on the dwell-time theory. However, the application of dwell-time logic often encounters a practical limitation: conservatism. The theoretical lower bound on the dwell time, $\tau_D$, typically depends on the transient characteristics of the system matrices. In [12] these bounds are computed using the condition number of the eigenvector matrices or crude estimates of the matrix exponential norm of the system's transition matrix. Such methods frequently yield prohibitive dwell-time requirements when applied to complex systems, forcing the system to remain in a sub-optimal configuration longer than necessary, thereby jeopardizing performance.

This paper addresses this problem. A less conservative method for computing the minimal admissible dwell time is proposed. We bridge the gap between the norm-bound approach [12] and the Multiple Lyapunov Function (MLF) framework. By leveraging Linear Matrix Inequalities (LMIs), tighter bounds on the transient behaviour of the switched system are derived. This allows for a mutual optimization of the controller/observer pairs to minimize $\tau_D$, ensuring rapid fault recovery while guaranteeing global stability. The proposed method is validated on the F-8 Crusader flight benchmark [13], demonstrating a significant reduction in the computed dwell time compared to standard norm-bound approache. The paper is structured as follows : Section II provides the necessary theoretical background on dwell-time stability for switched linear systems. Section III presents the main theoretical results, including the connection between norm-bound and MLF approaches and the proposed LMI-based algorithm for dwell-time computation. Finally, in Section IV the developed theory is applied to the supervisory FTC of the F-8C aircraft, showcasing the practical benefits of the proposed method.

## II. Background on dwell-time stability of switched systems

This section presents the necessary theoretical background on dwell-time stability for switched linear systems required for the understanding of the developments given in this paper. Consider a switched linear system arising from the supervisory control of a plant subject to faults. The closed-loop dynamics are described by:

$$\dot{x}(t) = A_{\sigma(t)}x(t) \tag{1}$$

where $x(t) \in \mathbb{R}^n$ is the state vector and $\sigma(t) : \mathbb{R}^+ \to \mathcal{P} = \{1, \ldots, N\}$ is the piecewise constant switching signal. The

†Corresponding author. [1]:IMS lab., Univ. Bordeaux, Bordeaux INP, CNRS (UMR 5218), 33405 Talence, France., {matteo.gouzien,david.henry}@u-bordeaux.fr; [2]: DTIS, ONERA, Universit'e de Toulouse, 31000, Toulouse, France. sergio.waitman@onera.fr

matrices $\{A_i\}_{i\in\mathcal{P}}$ are assumed to be Hurwitz. The switching instants are denoted by the sequence $\{t_k\}_{k\in\mathcal{I}}$, with $t_0 = 0$. Consequently, the switching sequence satisfies:

$$\forall k \in \mathcal{I}, \forall t \in [t_k, t_{k+1}), \quad \sigma(t) = \sigma(t_k) \tag{2}$$

*Assumption 1 (State continuity):* The state trajectory is assumed to be continuous at switching instants, i.e., $x(t_k^-) = x(t_k^+)$ for all $k \in \mathcal{I}$.

Stability of the system (1) is not guaranteed merely by the stability of individual subsystems. Fast switching between stable subsystems might induce divergence due to transient behaviours that can increase the state norm. Therefore, waiting in the exponentially decreasing phase before switching again is relevant. Liberzon and Hespanha [10] exposed a dwell-time constraint consisting of imposing a minimum delay between two switches.

*Definition 1 (Dwell time constraint):* A switching sequence $\sigma$ is said to respect a dwell time $\tau_D > 0$ if:

$$\forall k \in \mathcal{I}, \quad t_{k+1} - t_k \geq \tau_D.$$

The whole complexity of this approach lies in the computation of a minimal bound on $\tau_D$ that guarantees the global exponential stability of the switched system. Two main approaches exist in the literature: one based on bounding $\|e^{A_i t}\|$ directly, and another based on the Multiple Lyapunov Functions (MLF).

### A. The Norm-Bound Approach

According to [10], [12], we assume the transient behaviour is bounded by an exponential envelope.

*Assumption 2 (Exponential Bound):* Suppose there exist scalars $\alpha > 0$ and $\beta \geq 1$ such that ($\|.\|$ refers to the 2-norm):

$$\forall i \in \mathcal{P}, \quad \left\|e^{A_i t}\right\| \leq \beta e^{-\alpha t} \tag{3}$$

A dwell-time condition ensuring exponential stability of the switched system is given.

*Theorem 1 (Norm-Bound Dwell Time):* If the switching sequence respects a dwell time $\tau_D$ satisfying:

$$\tau_D > \frac{\ln(\beta)}{\alpha} \tag{4}$$

then the switched system is exponentially stable.

The following developments recall briefly the proof established in [10], [12] as some materials are required for subsequent developments.

*Sketch of proof:* Let $k \in \mathcal{I}$. Then between two switches, the norm of the state exponentially decays $\forall t \in [t_k, t_{k+1})$:

$$\begin{aligned}\|x(t)\| &\leq \beta e^{-\alpha(t-t_k)}\|x(t_k)\| \\ &\leq \beta^{k+1} e^{-\alpha t}\|x(0)\|\end{aligned} \tag{5}$$

If the switching sequence respects a dwell time of $k \leq \frac{t_k}{\tau_D} \leq \frac{t}{\tau_D}$. The norm of the state can be bounded as:

$$\|x(t)\| \leq \beta e^{\left(\frac{\ln(\beta)}{\tau_D} - \alpha\right)t}\|x(0)\| \tag{6}$$

If $\tau_D \geq \frac{\ln(\beta)}{\alpha}$, we have $\ln(\beta)/\tau_D - \alpha \leq 0$, leading to the exponential stability of the switching system. ■

The most straightforward way to find $\alpha$ and $\beta$ is to use the Jordan decomposition of $A_i$:

- $\alpha$ can be chosen as the minimal decay rate among the subsystem : $\alpha = -\max\{\mathrm{Re}(\lambda_i) \in \mathrm{Sp}(A_i),\ i \in \mathcal{P}\}$.
- $\beta$ can be chosen as the maximal condition number of the eigenvector matrices : $\beta = \max\{\|V_i\|\|V_i^{-1}\|,\ i \in \mathcal{P}\}$ where $V_i$ is the matrix of eigenvectors of $A_i$.

In Section IV-B, we will see that this approach may lead to a conservative bound for $\tau_D$, especially when $V_i$ is ill-conditioned due to large dimensions of the matrices $A_i$.

### B. The Multiple Lyapunov Function (MLF) Approach

Alternatively, stability can be analysed using Multiple Lyapunov Functions (MLF), as first introduced in [10]. This method involves constructing a set of Lyapunov functions, one for each subsystem, and analysing their behaviour during switching events. In this paper, we use quadratic functions, though more general Lyapunov candidates offer potential for further reducing conservatism.

*Assumption 3 (MLF Properties):* Suppose there exist $\eta > 0, \mu \geq 1$ and a set of symmetric positive definite matrices $\{P_i > 0, i \in \mathcal{P}\}$ such that:

$$\forall i \in \mathcal{P}, \quad \begin{cases} A_i^\top P_i + P_i A_i \leq -\eta P_i \\ P_i \leq \mu P_j, \quad \forall j \in \mathcal{P}, j \neq i \end{cases} \tag{7}$$

The following theorem can then be stated [10] :

*Theorem 2 (MLF Dwell Time):* The switched system is exponentially stable if the dwell time satisfies:

$$\tau_D > \frac{\ln(\mu)}{\eta} \tag{8}$$

The following developments recall briefly the proof reported in [10], some material being required for subsequent developments.

*Sketch of proof:* $\forall k \in \mathcal{I}$, $\forall t \in [t_k, t_{k+1})$, we have :

$$\begin{aligned}V(t) = V_{\sigma(t_k)}(t) &\leq e^{-\eta(t-t_k)} V_{\sigma(t_k)}(t_k^+) \\ &\leq \mu e^{-\eta(t-t_k)} V_{\sigma(t_{k-1})}(t_k^-) \leq \mu^k e^{-\eta t} V(0) \\ &\leq e^{\left(\frac{\ln(\mu)}{\tau_D} - \eta\right)t} V(0)\end{aligned} \tag{9}$$

■

In the literature, the condition (7) is often used. Nevertheless, it is rarely explained how to find the optimal pair $(\mu, \eta)$ (with respect to the minimal dwell time) such that the LMI system has a solution. This motivated the work reported in this paper.

## III. A less conservative dwell-time bound

### A. Bridging the gap between the two bounds

In the context of supervisory FTC, this work aims to tighten minimal dwell-time bound. While existing theories, such as those in [11], [12], rely on norm-bound formulations (3) that often yield overly conservative results. The approach based on LMIs seeks to enable faster switching between modes. This is crucial to avoid prolonged operation in sub-optimal configuration that compromise performance. The following establishes a connection between the two approaches. Note that the differences between the two approaches are:

- Bounding $\|e^{A_i t}\|$ relies on finding an exponential envelope. This means that the dwell-time definition relies mainly on the maximal transient value $\beta$ and the minimal decay rate $\alpha$.
- The MLF is a piecewise strictly exponentially decreasing signal with discontinuities at the switching instants. So, the exponential bound relies on the worst jump value $\mu$ and the minimal exponential decay rate $\eta$.

Let $\bar{\lambda}$ and $\underline{\lambda}$ be respectively the maximal and minimal eigenvalues of the Lyapunov matrices $\{P_i, i \in \mathcal{P}\}$, it follows that:

$$\forall t \geq 0,\ \underline{\lambda}\|x(t)\|^2 \leq V(t) \leq \bar{\lambda}\|x(t)\|^2 \tag{10}$$

Then, a new bound on $\|x(t)\|$ can then be derived from (9):

$$\forall t \in [t_k, t_{k+1}), \quad \|x(t)\| \leq \sqrt{\frac{\bar{\lambda}}{\underline{\lambda}}}(\sqrt{\mu})^k e^{-\eta t/2}\|x(0)\| \tag{11}$$

It follows by identification with (5) $\alpha = \frac{\eta}{2}, \beta = \sqrt{\mu}$, and consequently:

$$\tau_D > \frac{2\ln(\sqrt{\mu})}{\eta} = \frac{\ln(\mu)}{\eta} \tag{12}$$

### B. LMI-Based Algorithm

From (7), it is quite straightforward to see that the search of the minimal value of $\tau_D$ turns to the minimization of the ratio $\ln(\mu)/\eta$ such that following problem is feasible.

$$Pb(\eta,\mu):\ \forall i \in \mathcal{P}, \begin{cases} A_i^\top P_i + P_i A_i \leq -\eta P_i \\ P_i > 0 \\ P_i \leq \mu P_j,\ \forall j \in \mathcal{P}, j \neq i \end{cases} \tag{13}$$

Then, the problem can be reformulated as the following optimization problem:

$$\underset{\eta,\mu}{\text{minimize}} \left(\frac{\ln(\mu)}{\eta}\right) \text{ subject to } Pb(\eta,\mu) \text{ is feasible.} \tag{14}$$

To solve this problem, Algorithm 1 is proposed. Key ingredients of Algorithm 1 are as follows: The decay rate $\eta$ has a maximal bound when no jump constraint is considered. The first inequality of the LMI system (13) concerning the exponential decay rates gives:

$$(A_i + \frac{1}{2}\eta I)^\top P_i + P_i(A_i + \frac{1}{2}\eta I) < 0 \tag{15}$$

Thus, $(A_i + \frac{1}{2}\eta I)$ is Hurwitz for all $i \in \mathcal{P}$. This implies:

$$\eta \leq -2\max\{\mathrm{Re}(\mathrm{Sp}(A_i)),\ i \in \mathcal{P}\} = 2\alpha. \tag{16}$$

As the jump constraint only introduces additional restrictions, the maximal decay rate $\eta$ such that $Pb(\eta,\mu)$ has a solution is upper bounded by $2\alpha$. According to Algorithm 1, a list of test values $\{\eta_k \in (0, 2\alpha]\}$ is considered. For each $\eta_k$, a bisection search is used to find the minimal $\mu_k^\star$ such that $Pb(\eta_k, \mu_k^\star)$ is feasible. This leads to the minimal possible ratio $\ln(\mu_k)/\eta_k$.

**Algorithm 1** Optimal Dwell-Time LMI-based Algorithm

**Require:** System matrices $\{A_i\}_{i\in\mathcal{P}}$, Discretization resolution $N_{grid}$, Bisection tolerance $\epsilon$, Upper bound $\mu_{max}$.
**Ensure:** Optimal decay rate $\eta^*$, optimal jump $\mu^*$, and minimal dwell-time $\tau_D^*$.

```
Step 1: Discretization
Compute max decay: α ← −max{Re(Sp(A_i)), i ∈ P}
Define test set: H ← { k · 2α/N_grid | k = 1, ..., N_grid }
Initialize global minimum: τ*_D ← ∞
Step 2: Iterative Search
for each η_k ∈ H do
    Find μ_low such that Pb(η_k, μ_low) is not feasible
    Find μ_high such that Pb(η_k, μ_high) is feasible
    while (μ_high − μ_low) > ε do
        μ_test ← (μ_high + μ_low)/2
        Check LMI Feasibility Pb(η_k, μ_test):
        if Feasible then
            μ*_k ← μ_test
            μ_high ← μ_test
        else
            μ_low ← μ_test
        end if
    end while
    Update Global Optimum
    Compute current dwell time: τ_curr ← ln(μ*_k)/η_k
    if τ_curr < τ*_D then
        τ*_D ← τ_curr
        η* ← η_k
        μ* ← μ*_k
    end if
end for
return (η*, μ*, τ*_D)
```

## IV. Application to a F-8C aircraft

This section is devoted to the application of the theory presented in Section III, to the FTC problem of the F-8C crusader aircraft performing a coordinated turn, when control surfaces failures occur. In particular, we expose the trade-off that exists between decay rate and Lyapunov functions jump for the determination of the minimal dwell-time value.

### A. Problem statement

The lateral dynamic equations of the F-8C crusader can be found in [13]. In this work, uncertainties in mass, inertia, and aerodynamic coefficients are considered as in [13]. In terms of failures, the aircraft is assumed to be subject to left or right ailerons stuck, during a coordinated turn. As demonstrated in [13], the aircraft dynamics corresponding to such a scenario can be modelled according to three different state-space models $(A, B_i, C), i \in \mathcal{P} = \{1, 2, 3\}$, such that:

$$G_1(s) = C(s\mathbb{I} - A)^{-1}B_1 \quad \text{(fault-free case)} \tag{17a}$$
$$G_2(s) = C(s\mathbb{I} - A)^{-1}B_2 \quad \text{(left aileron failure)} \tag{17b}$$
$$G_3(s) = C(s\mathbb{I} - A)^{-1}B_3 \quad \text{(right aileron failure)} \tag{17c}$$

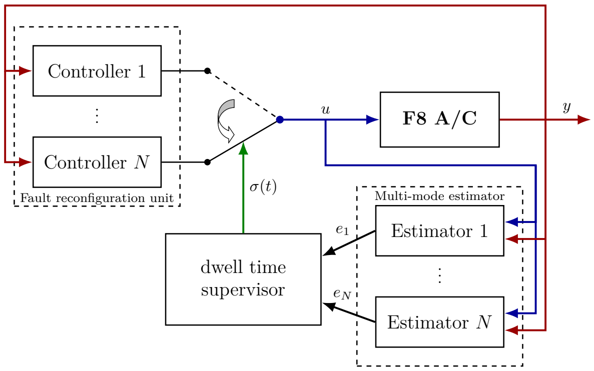


Fig. 1. The dwell-time FTC scheme.

The state vector is defined as $x = [p, r, \beta, \phi]^\top$ where $p$ is the roll rate, $r$ the yaw rate, $\beta$ the sideslip angle, and $\phi$ the bank angle. We assume that only the sideslip $\beta$, and bank angle $\phi$ are measured. The signal $\rho(t)$ denotes the operating mode of the system at time $t$. The dwell-time FTC scheme is depicted in Figure 1. As it can be seen, it relies on three main functions: the controllers, the multi-mode estimator and the dwell time supervisor.

For each mode $i \in \mathcal{P}$, a (stable) $H_\infty$ controller $K_i$ is built such that (see [13] for details about the design of $K_i$):

$$K_i(\gamma) : \begin{cases} \dot{\xi}_i(t) = A_{ci}(\gamma)\xi_i(t) + B_{ci}(\gamma)y(t) \\ u_i(t) = C_{ci}(\gamma)\xi_i(t) + D_{ci}(\gamma)y(t) \end{cases} \tag{18}$$

Each controller $K_i$ is parametrised by a scalar $\gamma$, introduced to vary the bandwidth of the $ith$ closed-loop. This parameter will be used later to derive the minimal dwell time. We recall that the objective we pursue, is to derive the optimal triplet "controllers / estimators / dwell-time supervisor".

The multi-mode estimator consists of Luenberger-like observers designed for each operating mode of the system. The observer dynamics for mode $i$ are given by:

$$\dot{z}_i = Az_i + B_i u + \varsigma_i + L_i(y - Cz_i), \; i \in \mathcal{P} \tag{19}$$

where $L_i$ are designed such that $A - L_iC$ are Hurwitz. We define a parameter $\kappa = -\max\{\mathrm{Re}\,(\mathrm{Sp}(A - L_iC))\}$ that constrains the observer poles relatively to the controller dynamics. It will be used (with $\gamma$) in Section IV-B for the minimal dwell time selection. The term $\varsigma_i$ is a design parameter. Note that the matched estimation error $e_\rho = x - z_\rho$ (i.e. when $i = \rho$) converges exponentially fast to zero, while the mismatched errors $e_i, i \neq \rho$ are influenced by the control input $u$, leading to a complex evolution.

Following the setup illustrated in Fig.1, the dwell-time supervisor is responsible for selecting the appropriate controller $K_{\sigma(t)}$ based on the minimal estimation error (in the $l_2$ norm-sense). It is defined for $k \geq 0, t_0 = 0$ by [12] :

$$\begin{aligned} t_{k+1} &= \arg \inf_{t \geq t_k + \tau_D} \left\{ \left\| Ce_{\sigma(t_k)}(t) \right\| > \left\| Ce_j(t) \right\|, j \in \mathcal{P} \backslash \{\sigma(t_k)\} \right\} \\ \sigma(t_k) &= \arg \min_{j \in \mathcal{P}} \left\| Ce_j(t_k) \right\|, \sigma(t) = \sigma(t_k), \forall t_k \leq t \leq t_{k+1} \end{aligned} \tag{20}$$

where $t_k, k \geq 0$ are the switching instants. For $t_0 = 0$, the switching signal is initialized as $\sigma(0) = \arg \min_{1 \leq j \leq 3} \|Ce_j(0)\|$ and the rule (20) is used for all time instants $t_k, k \geq 0$.

In accordance with the developments presented in [12], the closed-loop dynamics of the complete system (plant + controllers + observers) can be expressed as an "injected system" first introduced in [10], considering the estimation error $e_\sigma(t)$ as an input (for ease of reference, the same notations as in [12] are used):

$$\dot{\Psi}_{\sigma(t)}(t) = W_{\sigma(t),\rho(t)}\Psi_{\sigma(t)}(t) + V_{\sigma(t),\rho(t)}Ce_{\sigma(t)}(t) \tag{21}$$

Here, $\Psi_\sigma = [z_\sigma^\top, \xi_\sigma^\top, x^\top, z_1^\top, \ldots, z_N^\top, \xi_1^\top, \ldots, \xi_N^\top]^\top$ is the augmented state of the complete system. $W_{\sigma(t),\rho(t)}$ is a lower triangular matrix which has the form (see [11], [12])

$$W_{\sigma(t),\rho(t)} = \begin{bmatrix} H_{\sigma(t)} & 0 & 0 & 0 \\ \square & A\text{-}LC & 0 & 0 \\ \square & \square & A_{obs} & 0 \\ \square & \square & \square & A_{ctr} \end{bmatrix} \tag{22}$$

where $H_{\sigma(t)}$ is the matrix of the closed-loop dynamics of the controller $K_{\sigma(t)}$ on the plant in mode $\sigma(t)$, $A_{obs}$ is the block-diagonal matrix of all the observer dynamics $(A - L_iC), i \in \mathcal{P}$, and $A_{ctr}$ is the block-diagonal matrix of all the controllers dynamics $A_{ci}, i \in \mathcal{P}$. The matrix $V_{\sigma(t),\rho(t)}$ captures the influence of the observer error on the injected system dynamics. The notation "$\square$" represents sub-matrices that are not explicitly detailed here for brevity. Using permutation matrices $T_i$ such that $\Psi(t) = T_{\sigma(t)}\Psi_{\sigma(t)}(t)$ where $\Psi(t)$ is a common state vector defined by $\Psi(t) = [x^\top, z_1^\top, \ldots, z_N^\top, \xi_1^\top, \ldots, \xi_N^\top]^\top$, it follows that:

$$\dot{\Psi}(t) = \tilde{W}_{\sigma(t),\rho(t)}\Psi(t) + \tilde{V}_{\sigma(t),\rho(t)}Ce_{\sigma(t)}(t) \tag{23}$$

where $\tilde{W}_{\sigma(t),\rho(t)} = T_{\sigma(t)}W_{\sigma(t),\rho(t)}T_{\sigma(t)}^\top$ and $\tilde{V}_{\sigma(t),\rho(t)} = T_{\sigma(t)}V_{\sigma(t),\rho(t)}$.

Following the results stated in [12], the stability of the switched system (23) depends only on the left part of (23), which has the form of (1). Thus, the theoretical results stated in Section III can be applied to derive the smallest dwell-time value. More precisely, since $\tilde{W}_{\sigma,\rho}$ depends explicitly on $\gamma$ which determines the bandwidth of the closed loops and because $\tau_D$ depends on $\kappa$ that fixes the poles of the multi-estimator, the objective is to determine the optimal pair $(\gamma^*, \kappa^*)$ that leads to the minimal value of $\tau_D$. For that purpose, the MLF and norm-based approaches are compared, the MLF problem being solved with Algorithm 1.

### B. Mutual Optimization for minimal dwell-time

The faster the controllers and observers are, the more aggressive the closed-loop dynamics will be, which may lead to larger transients during switching events. This can increase the required dwell time. Conversely, slower controllers and observers may result in smaller transients but lower decay rates, compromising performance. Therefore, there is a trade-off between controller/observer dynamics and the dwell time. For our application case in view of the desired closed-loop dynamics, the range of $\gamma$ and $\kappa$ are selected to be $[0.2, 1]$ and $[20, 40]$, respectively.

*1) Influence of the controller speed:* To analyse the influence of $\gamma$ on the dwell time, the multi-estimator dynamics is fixed to $\kappa = 30$ rad/s. For $\gamma \in \{0.2, 0.4, 0.86, 0.96\}$, we compute the pairs $(\eta_k, \mu_k^\star)$ referred to in Algorithm 1 and the associated dwell time $\tau_{D_k}^\star = \ln(\mu_k^\star)/\eta_k$. The results are shown in Figure 2. As it can be seen, for a given $\gamma$, $\mu_k^\star$ and $\eta_k$ increase. Indeed, the problem $Pb(\eta_k, \mu)$ becomes more constrained as $\eta_k$ increases, leading to larger values of $\mu_k^\star$. The associated dwell time $\tau_{D_k}$ converges to a minimum value when $\eta_k$ tends to its maximal value. For this choice of $\kappa$ the minimal obtained dwell time is 2 s for $\gamma = 0.96$.

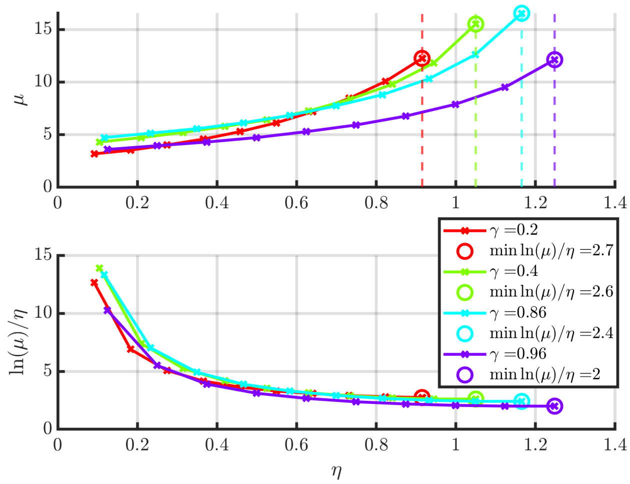


Fig. 2. Influence of $\gamma$ on the optimal $(\eta, \mu)$ and dwell time $\tau_D$ for $\kappa = 30$.

*2) Influence of the observer speed:* Let us now fix the controller speed parameter to $\gamma = 0.96$. The multi-estimator dynamics vary according to $\kappa \in \{20, 30, 40\}$. The results are shown in Figure 3. On the first subplot, the trend is similar to the previous case. Moreover, the obtained results are the same for all the $\kappa$ values. This means that the multi-estimator dynamics does not influence the solution of the LMI problem $Pb(\eta, \mu)$ and the resulting dwell-time value. This is due to the fact that the eigenvalues of the observer dynamics $A - L_iC$ are chosen to have poles faster than the closed-loop dynamics $H_i$. Thus, the eigenvalues of $A - L_iC$ do not impact the slowest decay rate $\alpha$ of $W_{i,j}$ which mainly depends on $H_i$. However, the $L_i$ matrix could have an impact on the highest jump parameter $\mu$ as it also appears in the lower off-diagonal terms of $W_{i,j}$. However, for our application case, Figure 3 shows that this influence is negligible for $\gamma = 0.96$.

*3) Combined influence of $\gamma$ and $\kappa$ and comparison with norm-based dwell time computation:* We now vary simultaneously $\gamma$ and $\kappa$. For each pair the associated dwell time value is computed using both Algorithm 1 and the norm-bound method, see Section II-A. Figure 4 shows the obtained $\tau_D$ surfaces as a function of $\gamma$ and $\kappa$. Black lines have been plotted at constant $\gamma$ values. As it can be seen, the values of $\tau_D$ obtained with Algorithm 1 are significantly lower than those obtained with the norm-bound method. For the latter, the minimal dwell time value is 5.6 s for $\gamma = 0.96$ which is unacceptable for a fault-tolerant control law for

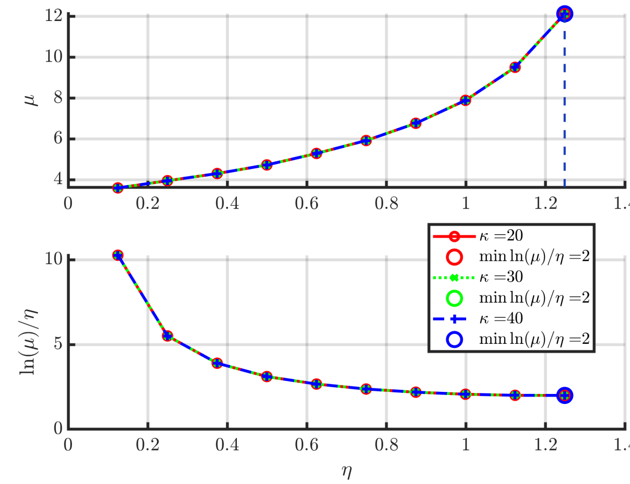


Fig. 3. Influence of $\kappa$ on the optimal $(\eta, \mu)$ and dwell time $\tau_D$ for $\gamma = 0.96$.

a fighting aircraft performing a lateral manoeuvrer. If the supervisory scheme fails to select the adequate controller leading to an unstable closed-loop, which turns out to be the case, the dwell-time supervisor has to wait $\tau_D = 5.6$ s before engaging a new controller. It should be pointed out that, due to numerical conditioning problems of the matrices $V_i$, the values of $\kappa$ influence the values of $\tau_D$ for the case of the norm-bound approach.

On the other hand, the proposed LMI-based method yields a minimal dwell time of 2 s for $\gamma^\star = 0.96$. This value is more acceptable in practice and allows the design of a responsive supervisory FTC system. Note on the left-hand plot in Figure 4, that this approach exhibits more robust numerical properties against the variations of $\kappa$, making any value of $\kappa$ fast enough admissible. This result simplifies the optimization process by making it one-dimensional in $\gamma$. In the following, the value of $\kappa^\star = 30$ rad/s is selected.

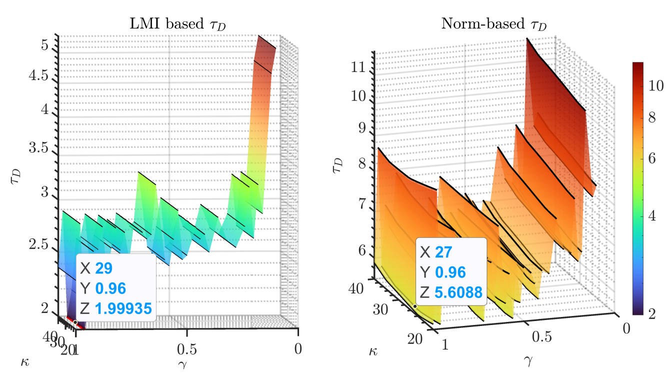


Fig. 4. Combined influence of $\gamma$ and $\kappa$ on $\tau_D$ for the two methods.

## C. Simulation Results

The performance of the derived FTC scheme is finally assessed via a nonlinear simulation. The test scenario imposes a coordinated yaw turn, with a reference trajectory imposed on the bank angle $\phi(t)$, and a sideslip angle $\beta(t)$ fixed to zero.

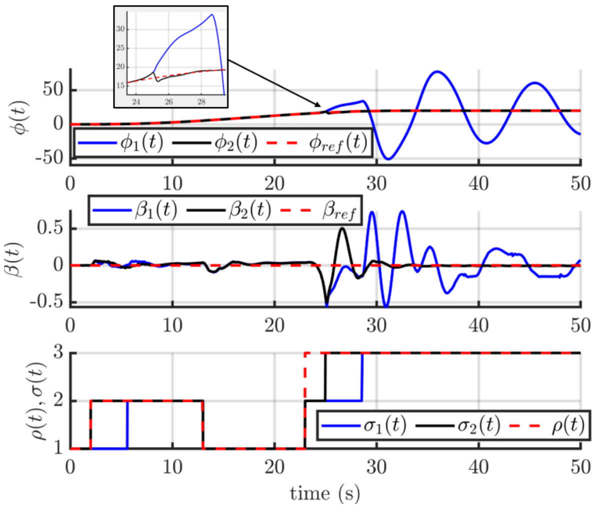


Fig. 5. $\phi(t)$, $\beta(t)$ with the reference signals (in deg.), switching sequences of the plant $\rho(t)$ and of the dwell-time supervisor $\sigma(t)$ with norm-based $\tau_D = 5.6s$ (blue curves with index $_1$) and LMI based $\tau_D = 2s$ (black curves with index $_2$).

The simulation is conducted with a precision of the angle sensors fixed to $\pm 0.1°$, and the following fault scenario :

- At $t = 0$ $s$, the system starts in nominal mode.
- At $t = 5$ $s$, the right aileron is locked in place.
- At $t = 20$ $s$, the right aileron is back healthy.
- At $t = 25$ $s$, the left aileron is locked in place.

Note that this scenario is not realistic in practice, but allows to highlight the functioning of the proposed FTC scheme. Figure 5 illustrates the behaviour of the bank $\phi(t)$ and sideslip $\beta(t)$ angles. Figure 6 illustrates the true control surface commands: left aileron $da_l(t)$, right aileron $da_r(t)$, and rudder $dn(t)$, where we can see the lock-in-place faults in the ailerons. The switching sequence $\sigma(t)$ determined by the dwell-time supervisor is also presented with the operating mode $\rho(t)$. As it can be noted, the supervisor selects mismatched controllers at some instants but the dwell time constraint ensures the stability of the overall system. This induces temporarily degraded tracking performance on $\phi(t)$ and oscillation on the sideslip angle $\beta(t)$. However, the system quickly recovers when the matched controller is selected. The sideslip angle $\beta(t)$ is kept close to zero. The results obtained from the norm-bound approach to compute $\tau_D$ are superposed as an illustration. Clearly, these results confirm the relevance of the proposed LMI-based approach to compute the minimal value of $\tau_D$.

## V. Conclusion

This paper proposed a method to reduce conservatism in the design of dwell-time supervisory fault-tolerant control solutions. By reinterpreting Multiple Lyapunov Function properties to derive optimal parameters for the norm-bound stability condition, an LMI-based algorithm is proposed. The application on the F-8 Crusader benchmark demonstrates a 64% reduction in dwell time, ensuring the closed-loop stability and greatly improving the responsiveness of the approach. Future work will focus on integrating a neural network into the multi-estimator to enhance its ability to accurately identify the operating mode.

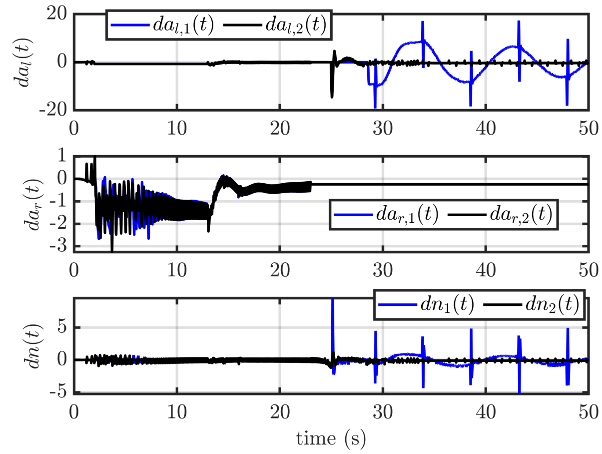


Fig. 6. Left $da_l$ and right $da_r$ aileron and rudder $dn$ commands (in deg.), with norm-based $\tau_D = 5.6s$ (blue curves with index $\square_1$) and LMI based $\tau_D = 2s$ (black curves with index $\square_2$).

## References


[1] S. X. Ding, *Advanced Methods for Fault Diagnosis and Fault-Tolerant Control*. Berlin, Heidelberg: Springer, 2021.

[2] İ. Gümüşboğa and A. İftar, "An integrated fault-tolerant control strategy for control surface failure in a fighter aircraft," *The Aeronautical Journal*, vol. 126, no. 1303, pp. 1568–1592, Sep. 2022.

[3] G. Magnani, M. Cassaro, J.-M. Biannic, H. Evain, and L. Burlion, "Quadrotor Fault-Tolerant Constrained Control Using Interval Contractor-Based Adaptive Reference Governor," *IEEE Transactions on Aerospace and Electronic Systems*, vol. 61, no. 2, pp. 1409–1421, Apr. 2025.

[4] H. Alwi, C. Edwards, O. Stroosma, and J. A. Mulder, "Fault Tolerant Sliding Mode Control Design with Piloted Simulator Evaluation," *Journal of Guidance, Control, and Dynamics*, vol. 31, no. 5, pp. 1186–1201, Sep. 2008.

[5] L. Liu, Y. Shen, and E. H. Dowell, "Integrated Adaptive Fault-Tolerant H Infinity Output Feedback Control with Adaptive Fault Identification," *Journal of Guidance, Control, and Dynamics*, vol. 35, no. 3, pp. 881–889, May 2012.

[6] M.-Z. Gao and G.-P. Cai, "Finite-time H $\infty$ adaptive fault-tolerant control for wing flutter of reentry vehicle subject to input saturation," *International Journal of Control, Automation and Systems*, vol. 15, no. 1, pp. 362–374, Feb. 2017.

[7] A. Antonakis and J.-M. Biannic, "Minimum-Drag Fault-Tolerant Aircraft Control Allocation via Online Lifting Line Calculation," *Journal of Aircraft*, vol. 61, no. 5, pp. 1428–1439, Sep. 2024.

[8] G. J. Ducard, *Fault-Tolerant Flight Control and Guidance Systems*, ser. Advances in Industrial Control. London: Springer London, 2009.

[9] J. Lan and R. J. Patton, "A decoupling approach to integrated fault-tolerant control for linear systems with unmatched non-differentiable faults," vol. 89, pp. 290–299.

[10] D. Liberzon, *Switching in Systems and Control*, ser. Systems & Control: Foundations & Applications. Boston, MA: Birkhäuser, 2003.

[11] J. Cieslak, D. Efimov, and D. Henry, "Transient management of a supervisory fault-tolerant control scheme based on dwell-time conditions," *International Journal of Adaptive Control and Signal Processing*, vol. 29, no. 1, pp. 123–142, Jan. 2015.

[12] D. Efimov, J. Cieslak, and D. Henry, "Supervisory fault-tolerant control with mutual performance optimization," *International Journal of Adaptive Control and Signal Processing*, vol. 27, no. 4, pp. 251–279, Apr. 2013.

[13] M. Gouzien, S. Waitman, and D. Henry, "A dwell-time approach for global optimal fault-tolerant control performance: an aeronautic case," in *2025 6th International Conference on Control and Fault-Tolerant Systems (SysTol)*, 2025, pp. 386–391.